

Optimal Liquid Desiccant Regeneration by a Low Cost Unglazed Air and Water Heating Collector

Abdul Qadir¹ and Peter Armstrong¹

¹Masdar Institute of Science and Technology, Abu Dhabi, United Arab Emirates

1. Abstract

System performance of a novel Liquid-Air Transpired Solar Collector (LATSC) and a falling film type, parallel plate liquid desiccant regenerator (LDR) using lithium chloride as the desiccant is evaluated. A brief overview of the LATSC is provided followed by the development of a numerical model for the LDR. The LATSC and LDR are then coupled and a sensitivity analysis is performed on the system. The combined LATSC-LDR system is optimized for typical Abu Dhabi weather conditions. It is found that at LiCl desiccant solution entering and leaving concentrations of 0.2 and 0.4 the optimal water thermal capacitance rate per unit collector area, air thermal capacitance rate per unit collector area, and desiccant mass flow rate per unit collector area are 38.655 W/m²K, 10.979 Wm²K, and 0.00016645 kg/s-m² respectively. The system efficiency under these conditions is almost 23%.

2. Introduction

Air conditioning is a large electricity user in hot and humid climates. For example over 60% of peak electricity use in Abu Dhabi city is attributed to cooling and 20% of annual electrical energy required for cooling is attributed to dehumidification (Ali, et al., 2011). It has been proposed that latent cooling loads can be economically addressed by thermally regenerated desiccant cycles (Lof, 1956, Threlkeld, et al., 1998). This allows for the separation of latent and sensible cooling functions and thus higher chilled water temperatures may be used to handle the sensible cooling load, decreasing the energy input to vapor compression chillers (Armstrong, et al., 2009) and absorption chillers (Threlkeld, Ramsey and Kuehn, 1998).

One potential regeneration heat source—the Liquid Air Transpired Solar Collector (LATSC)—has previously been described by Qadir and Armstrong (2011). The LATSC is a novel, low-cost, unglazed solar thermal collector which heats air and water simultaneously. Analysis of the LATSC application to desiccant regeneration is motivated by the fact that both hot water and air can be used to regenerate a liquid desiccant. The collector operates at maximum efficiency when the water flow is zero and air suction through the absorber plate is high while the regenerator efficiency is highest at high water flow rates. Furthermore the desiccant flow rate needs to be varied in order to regenerate the dilute desiccant solution (0.2 LiCl concentration) to a strong solution (0.4 LiCl concentration). Therefore the air, water and desiccant flow rates that maximize system performance must be determined for any given condition. This paper presents a brief overview of the LATSC model and develops a numerical model for a falling film type LDR. The LATSC and LDR are then coupled and performance of the combined system is optimized for typical Abu Dhabi conditions. Solar cooling systems based on the LATSC-LDR may be used for dehumidification only or may be combined with evaporative cooling to perform sensible cooling.

3. Method

LATSC Model. The LATSC (Qadir and Armstrong, 2011) consists of a uniformly perforated absorber plate with tubes bonded or integral to the plate such that water flows parallel to the air moving behind the plate and toward the top of the collector where both air and heated water exit. The LATSC can be thought of as a conventional transpired air heating collector (Kutscher, et al., 1993) but with addition of tubes or channels to heat water. Conversely, one can liken the LATSC to a conventional unglazed flat plate collector (Burch, et al., 2005) but with the addition of perforations on the plate and a plenum behind the absorber plate to allow movement of the air from the front to

behind the plate and then to the outlet duct. In operation, water is heated in the tubes while air is sucked through the absorber plate and is heated at the same time. Figure 1 shows the schematic of the LATSC highlighting the differential element dy . For simplicity and due to symmetry, the small shaded patch in the bottom left corner of the collector is used to show the heat and mass balance on the differential element and is shown magnified in Figure 2.

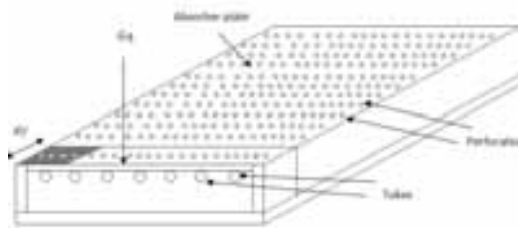


Figure 1: Schematic of LATSC

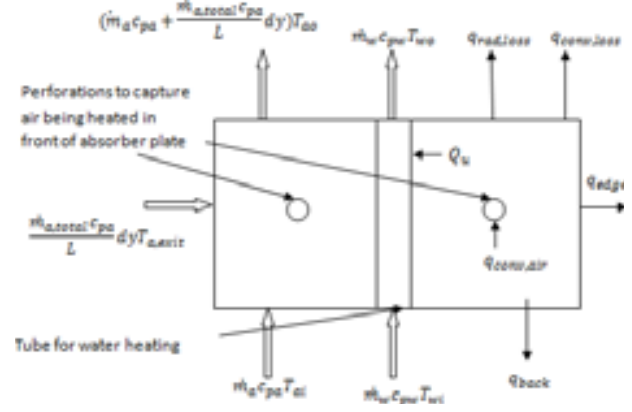


Figure 2: Energy balance on differential area of absorber plate.

The heat and mass balance on the differential element lead to the formulation of three ordinary differential equations (ODE) which determine the temperature of water, temperature of air and mass of air along the length of the collector (assuming uniform suction along the plate) respectively. These ODEs are:

$$\dot{m}_w c_{pw} \frac{dT_w}{dy} = Q_u \quad (1)$$

$$(\dot{m}_{ai} + \Delta \dot{m}_a) \frac{dT_a}{dy} = \frac{\dot{m}_{a,tot}}{L} [(1 - \epsilon_{hx}) T_{amb} + \epsilon_{hx} T_{pl} - T_{ai}] \quad (2)$$

$$\frac{d\dot{m}_a}{dy} = \frac{\dot{m}_{a,tot}(y)}{L} \quad (3)$$

The three ODEs must be solved simultaneously for all dy to obtain the outlet air and water temperatures. Collector efficiency is defined as the ratio of the total thermal energy gain of the air and water to the solar radiation incident on the collector. It is given in mathematical form as:

$$\eta_{coll} = \frac{\dot{m}_a c_{pa} (T_{ao} - T_{ai}) + \dot{m}_w c_{pw} (T_{wo} - T_{wi})}{G * A_c} \quad (4)$$

LDR Model. A liquid desiccant regenerator (LDR) model was developed to test the performance of the LATSC for one of its potential applications. For this purpose a simple model was built with the following assumptions:

1. Steady state operation of the LDR
2. Enthalpy of dilution neglected because a small amount of water is added/taken from each control volume
3. Laminar, non wavy, fully wetted flow of liquid desiccant over parallel plate
4. Constant properties of air, water and desiccant in a control volume
5. Fully mixed desiccant film (no thermal gradient, no concentration gradient in x-direction)

The falling film configuration can operate with close approach temperatures and high thermodynamic efficiencies. It also allows for internal heating of the desiccant by hot water and simultaneous regeneration of the desiccant by contact with hot air, providing the opportunity for the use of both heated air and water from the LATSC.

The regenerator consists of many parallel plates containing internal channels through which the hot water flows from top to bottom. Desiccant is distributed uniformly at the top of the regenerator plate and it flows down the air side of the plate as a thin film. Air is injected from the bottom and it moves towards the top giving the LDR a counter flow configuration. There exists a plane of symmetry at the center of each air side and water side channel about which symmetry of physical properties and chemical composition of the water, air and desiccant are encountered in the negative and positive x-direction. A heat and mass balance is first performed on a control volume of the regenerator shown in Figure 3.

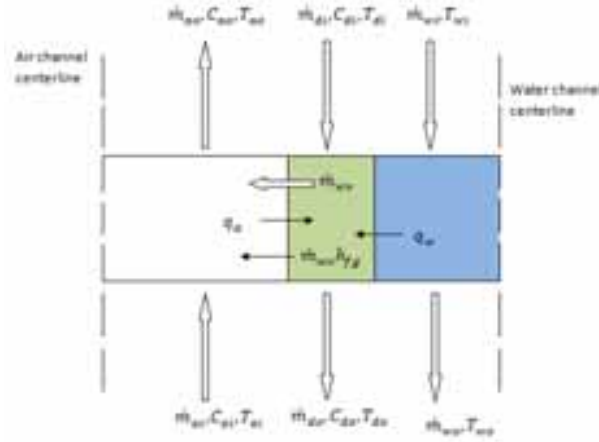


Figure 3: Heat and Mass balance on a differential element of the LDR.

The three mass balance equations for each control volume are:

$$\text{for the air:} \quad \dot{m}_{ao} = \dot{m}_{ai} + \dot{m}_{wv} \quad (5)$$

$$\text{for the desiccant:} \quad \dot{m}_{do} = \dot{m}_{di} - \dot{m}_{wv} \quad (6)$$

$$\text{and for the water:} \quad \dot{m}_{wo} = \dot{m}_{wi} \quad (7)$$

$$\text{where the mass of air is composed of dry air and moisture:} \quad \dot{m}_a = \dot{m}_{da} + \dot{m}_{da}\omega \quad (8)$$

Similarly the desiccant solution contains desiccant salt and water:

$$\dot{m}_d = \dot{m}_{ds} + \dot{m}_{wd} \quad (9)$$

The concentrations of water in air and in the desiccant solution must satisfy continuity for each control volume.

$$\text{The air humidity is:} \quad C_{ao} = \frac{C_{ai}\dot{m}_{ai} + \dot{m}_{wv}}{\dot{m}_{ao}} \quad (10)$$

$$\text{and the desiccant concentration is:} \quad C_{do} = \frac{C_{di}\dot{m}_{di} - \dot{m}_{wv}}{\dot{m}_{do}} \quad (11)$$

Finally the energy balances for the air, water and desiccant elements must be satisfied for each control volume. For the air stream element the energy balance is given by:

$$\dot{m}_{da,o}c_{pdao}T_{ao} + (\dot{m}_{da,i}\omega + \dot{m}_{wv})c_{pwv}T_{ao} = \dot{m}_{dai}(c_{pda,i} + \omega c_{pwv})T_{ai} - q_a + \dot{m}_{wv}c_{pwv}T_{di} \quad (12)$$

Equation (12) says that the airstream enthalpy out of the regenerator equals the airstream enthalpy in, plus the enthalpy of vapor from the desiccant, minus heat transferred to the desiccant. For the desiccant element we have:

$$\dot{m}_{do}c_{pdo}T_{do} = \dot{m}_{di}c_{pdi}T_{di} + q_a + q_w - \dot{m}_{wv}h_{fg} \quad (13)$$

Equation (13) says that the change in desiccant solution enthalpy is proportional to the sum of heat gains from the air and water, minus the enthalpy of evaporation of moisture rejected to the airstream. For the water element:

$$\dot{m}_{wo}c_{pwo}T_{wo} = \dot{m}_{wi}c_{pwo}T_{wi} - q_w \quad (14)$$

Equation (14) says that change in water temperatures is proportional to rate of heat transfer to the desiccant stream.

The correlation for heat transfer from air to the desiccant was developed by assuming a laminar, fully developed flow of air between the two parallel plates. The temperature of the plate at each element was assumed constant for which the Nusselt number (Nu_a) is 7.54 (Incropera, et al., 2006).

Similarly we assume that the water channel is in fully developed laminar flow with constant plate temperature over each element and the therefore Nusselt number for heat transfer from the water to the desiccant (Nu_w) is also 7.54.

Convection rates at the air-desiccant interface, q_a , and water-desiccant interface, q_w , are given by:

$$q_a = h_a(T_{ai} - T_{di})Wdy \quad (15)$$

where

$$h_a = \frac{Nu_a k_a}{D_{h,a}} \quad (16)$$

and

$$q_w = h_w(T_{wi} - T_{di})Wdy \quad (17)$$

where

$$h_w = \frac{Nu_w k_w}{D_{h,w}} \quad (18)$$

where the $D_{h,a}$, $D_{h,w}$ are the hydraulic diameters of the channels through which the air and water flow.

The mass transfer coefficient for water vapor transfer to the air stream can be estimated using the Chilton-Colburn analogy:

$$h_m = \frac{h_a}{\rho_a c_{pa}} \left(\frac{\alpha_a}{D_{a,wv}} \right)^{-2/3} \quad (19)$$

The water vapor mass transfer for each element can then be determined:

$$\dot{m}_{wv} = h_m \rho_a (C_{int} - C_{ai}) \quad (20)$$

C_{int} is the equilibrium water vapor concentration at the air-desiccant interface while C_{ai} is the water vapor concentration in the inlet air. The desiccant used for the regenerator analysis is lithium chloride and the properties of the desiccant-water solution are given by Conde (2004). Properties of air and air-water mixtures built in to EES are based on thermodynamic data developed by Hyland and Wexler (1983) and reported in handbooks ASHRAE(2009).

LDR Solving Procedure. The counter-flow configuration of the LDR means that the conditions at all nodes must be solved simultaneously. One simple approach is to split the regeneration process in to two cycles, A and B. In cycle A, the air temperature and concentration for each node are kept constant while the water and desiccant temperatures and concentrations are evaluated for each node. These values are then plugged in to the nodes of cycle B, while the air temperatures and concentrations are evaluated for each node. The process is repeated until the water vapor transferred to the air at each node is equal in both cycles (i.e. $\dot{m}_{wv}(i)_A = \dot{m}_{wv}(i)_B$ for all i as shown in Figure 4).

Combined Model. The model described above was combined with the LATSC model and simulated using Engineering Equation Solver (EES) to obtain the overall system efficiency ($\eta_{overall}$) for varying $(\dot{m}c_p)_{total}$ and $R_{\dot{m}cp}$. The overall system efficiency is:

$$\eta_{overall} = \eta_c \eta_{reg} \quad (21)$$

Where

$$\eta_{reg} = \frac{\dot{m}_{da} h_{fg} (\omega_{ao} - \omega_{ai})}{\dot{m}_a c_{pa} (T_{ao} - T_{ai}) + \dot{m}_w c_{pw} (T_{wo} - T_{wi})} \quad (22)$$

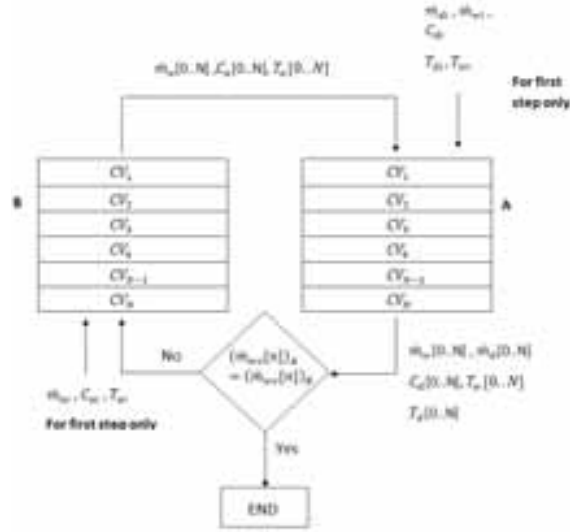


Figure 4: Flow chart of solving procedure for LDR

and η_c was defined in (4). The regeneration efficiency is the ratio of the energy used to evaporate water from the desiccant solution to the total energy provided by the LATSC. The overall system efficiency is the ratio of the energy used to evaporate the water from the desiccant solution to the incident solar radiation on the collector surface. It can also be expressed as the product of the regeneration efficiency and the collector efficiency.

The schematic of the coupled model is illustrated in Figure 5. There are separate loops for the flow of water, desiccant and air in the coupled system. The water and desiccant solution flow in a closed loop while the air and the moisture in the desiccant flow in an open loop. The air enters the collector at T_{amb} and leaves at mass flow rate \dot{m}_a . Air then moves to the regenerator at T_{ao} and in passing gains mass by evaporation of water from the desiccant, leaving the regenerator with a mass flow rate of \dot{m}_{ao} and temperature of $T_{ao,reg}$. The desiccant solution is pumped from the top of a stratified tank in-to the regenerator with a concentration of C_{di} , temperature T_{di} and mass flow rate \dot{m}_{di} . The desiccant solution loses mass in the regenerator as the water evaporates into the air stream leading to an exit temperature, T_{do} and concentration C_{do} , with mass flow rate \dot{m}_{do} .

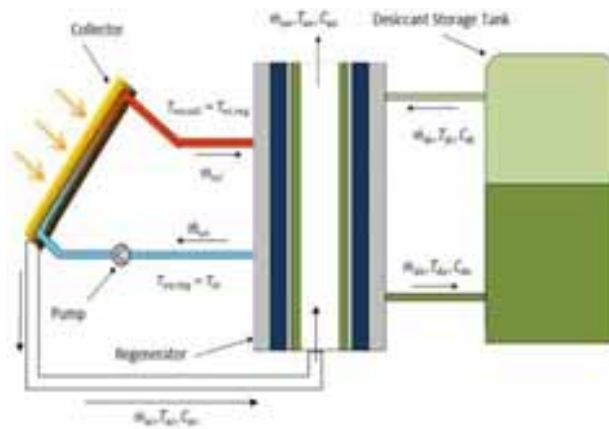


Figure 5: Schematic of LATSC coupled with LDR and an ideally stratified storage tank.

To simultaneously solve for collector and regenerator water outlet temperatures, the LATSC and LDR models are evaluated iteratively as shown in Figure 6.

The physical dimensions and inlet conditions of the regenerator are summarized in Table 1.

Table 1: Parameters and Inlet Conditions of the Regenerator

Parameter	Value
Plate height	0.5 m
Plate width	0.5 m
Plate spacing	0.005 m
Desiccant flow rate	0.000653 kg/s
Inlet desiccant concentration	0.2
Control volume height	0.001m
Number of control volumes	500

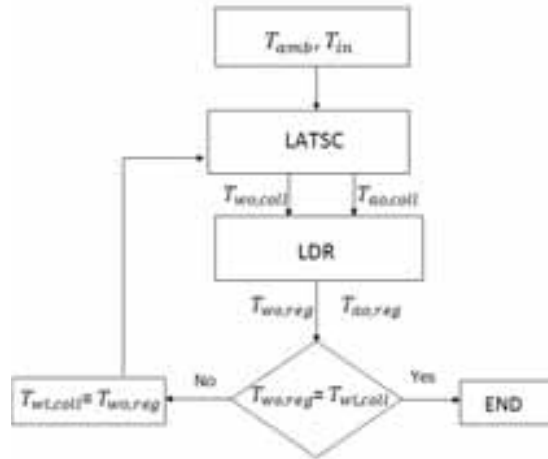


Figure 6: Flow chart for the LATSC-LDR coupled model.

4. Sensitivity Analysis

LATSC and LDR parameters are listed in Table 2. The total (air + water) thermal capacitance rate, $(\dot{m}c_p)_{total}$, was varied from $5\text{W/m}^2\text{K}$ to $25\text{W/m}^2\text{K}$ at five equal intervals. For each $(\dot{m}c_p)_{total}$, the air capacitance rate fraction, $R_{\dot{m}c_p}$, was varied from 0.2 to 0.9 in increments of 0.1 while operating conditions were kept constant at incident flux, $S = 800\text{ W/m}^2$, wind, $V_w = 3\text{ m/s}$ and $T_{amb} = 25^\circ\text{C}$. The desiccant mass flow rate was also kept constant at 0.000653 kg/s . Figures 7-9 show the variation of the collector, regenerator and overall efficiency with $R_{\dot{m}c_p}$ for different $(\dot{m}c_p)_{total}$ for the coupled system.

The collector efficiency tends to increase as $R_{\dot{m}c_p}$ is increased from 0.2-0.9 at a constant $(\dot{m}c_p)_{total}$. This is due to the large temperature drop for water across the regenerator when $R_{\dot{m}c_p}$ is increased, $((\dot{m}c_p)_w$ decreases), leading to a lower inlet water temperature supplied to the collector. On the other hand the regenerator efficiency tends to decrease with an increase in $R_{\dot{m}c_p}$. This is because higher water flow rates maintain a constant high temperature in the internally heated regenerator, leading to higher regeneration efficiencies. It should be noted that while the

temperature of the inlet water to the regenerator is higher at higher air thermal capacitance fractions, $R_{\dot{m}c_p}$ s, that temperature cannot be sustained along the length of the regenerator due to the constant heat transfer to the desiccant for regeneration. The variation of the collector water outlet temperatures or regenerator water inlet temperatures with $R_{\dot{m}c_p}$ at a different $(\dot{m}c_p)_{total}$ are shown in Figure 10.

Table 2: Geometric parameters, fluid properties and baseline conditions used in the sensitivity analysis

Property	Value
Length of collector (L)	2m
Width of collector (W)	1m
Plenum depth (D)	0.1m
Perimeter of plenum cross section	2.2m
Plate absorptivity	0.9
Plate emissivity	0.9
Hole diameter	0.00159m
Hole pitch (triangular pattern)	0.025m
Total free area of holes	0.00734 m ²

The overall efficiency is seen to increase with an increase in $R_{\dot{m}c_p}$ and to reach a maximum after which it tends to decrease. The maximum overall efficiency is achieved at different $R_{\dot{m}c_p}$ for different $(\dot{m}c_p)_{total}$. As $(\dot{m}c_p)_{total}$ increases, the $R_{\dot{m}c_p}$ at which the maximum efficiency is observed decreases. The trend observed can be explained by the preference of the regenerator for hot water over hot air and of the collector for an air suction rate just enough to suppress the majority of the convective losses so that the collector operates at a reasonable efficiency.

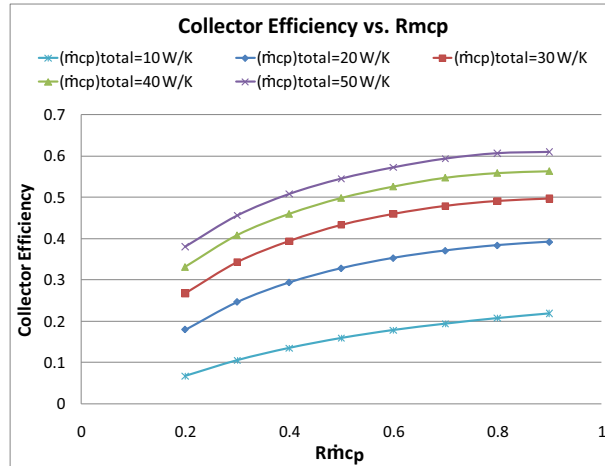


Figure 7: Collector Efficiency vs $R_{\dot{m}c_p}$ for coupled system

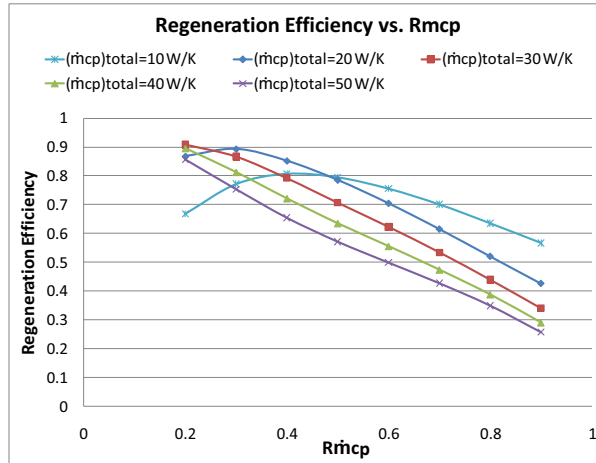


Figure 8: Regeneration Efficiency vs R_{mcp} for coupled system.

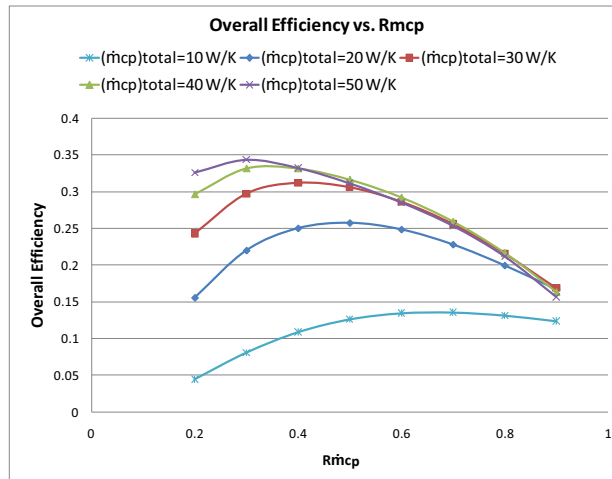


Figure 9: Overall Efficiency vs R_{mcp} for coupled system.

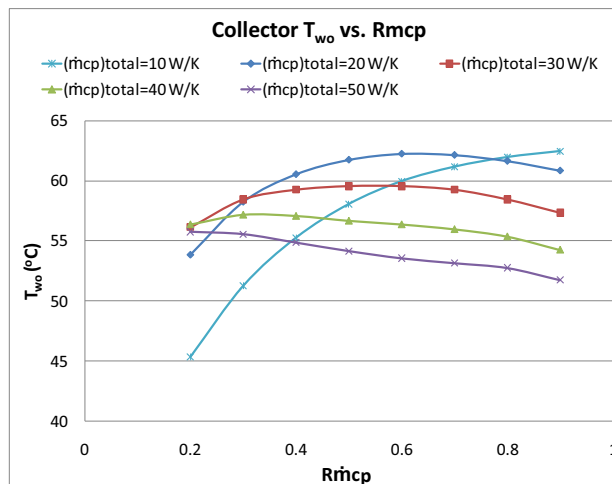


Figure 10: Collector water outlet/Regenerator water inlet temperature vs R_{mcp} .

5. Optimization

In the sensitivity analysis shown above, only 2 parameters (\dot{m}_{cpa} and \dot{m}_{cpw}) were varied to assess the sensitivity of the system to changes in these parameters. In practical applications, there are many more parameters that can be varied to optimize the system for different weather conditions. In this section the combined LATSC and LDR system is optimized according to typical weather conditions in Abu Dhabi.

Typical weather conditions were determined by assessing the weather data for one year in Abu Dhabi. The weather conditions that affect the performance of the combined collector-regenerator system are solar radiation, ambient temperature, wind speed and humidity. To determine these values for a typical Abu Dhabi day, TMY2(2005) (Remund, et al., 2003) data for Abu Dhabi were plotted on a histogram for each of the parameters with different equally sized bins depending on the variability of a particular parameter. For example solar radiation varies for most parts of the day between 300W/m^2 to over 1000W/m^2 while wind speed tends to range between 0 and 5 m/s. The range of values of the parameters and the bin sizes for the parameters are shown in Table 3.

Table 3: Frequency (hours/year) of Abu Dhabi weather used to select typical operating condition (Remund 2003)

Parameter	Range	Bin size	Below	Bin 1	Bin 2	Bin 3	Bin 4	Bin 5	Above
Solar Radiation on tilt (W/m^2)	100-900	200	4660	382	632	837	861	1088	300
Wind Speed(m/s)	1-5	1	2	725	1535	1799	1600	1186	1933
Humidity ($\text{kg}_w/\text{kg}_{da}$)	0.015-0.035	0.005	19	1804	2524	2142	1648	529	94
Ambient temperature ($^{\circ}\text{C}$)	20-45	5	203	1222	1759	2124	1732	1283	437

The typical condition selected for optimization is $S = 850\text{W/m}^2$, $V_w = 4$ m/s, $w = 0.02\text{kg}_w/\text{kg}_{da}$ and $T_{amb} = 27.5^{\circ}\text{C}$.

The objective of the optimization is to regenerate the liquid desiccant to a concentration of 0.4 while maximizing the desiccant flow rate. Thus an objective function, to be minimized, was defined as:

$$f(\text{objective}) = \frac{\text{abs}(C_{do}-0.4)}{\dot{m}_{di}} + \frac{1}{\dot{m}_{di} \cdot 1000} \quad (23)$$

The numerator in the first term is the absolute difference between the outlet desiccant concentration and the desired outlet desiccant concentration. Minimization of this term is vital since the desiccant outlet concentration is required to be 0.4. Thus this term is divided by \dot{m}_{di} , which is in the order of 10^{-4} . This ensures that the optimization solver brings the outlet desiccant concentration as close to zero as possible. The second term has the desiccant flow rate in the denominator to ensure that as the desiccant outlet concentration reaches 0.4, the optimizer focuses on maximizing the desiccant flow rate.

The optimum air and water thermal capacitance rates and desiccant mass flow rate per unit collector area were found using a genetic algorithm (MATLAB) for the typical condition (Table 4) and the system efficiency was 22.59%.

Table 4: Optimum mass flow and thermal capacitance rates per unit collector area

Inlet Condition	Value
Water capacitance rate	38.655 $\text{W/m}^2\text{-K}$
Air capacitance rate	10.979 $\text{W/m}^2\text{-K}$
Desiccant mass flow rate at LDR inlet per unit collector area	0.00016645 kg/s-m^2

6. Discussion

The increase in the collector efficiency with increasing $(\dot{m}c_p)_{total}$ and $R_{\dot{m}cp}$ is due to the large temperature drop for water across the regenerator when $R_{\dot{m}cp}$ is increased, ($(\dot{m}c_p)_w$ decreases), leading to a lower inlet water temperature supplied to the collector. The decreasing trend in the regenerator efficiency with increasing $R_{\dot{m}cp}$ is due to the lower flow rates of heated water in the regenerator, which lead to lower heat transfer to the desiccant in the regenerator, leading to lower regeneration efficiency. It should be noted that while the temperature of the inlet water to the regenerator is higher at higher $R_{\dot{m}cp}$ s, that temperature drops quickly as we move down the regenerator water channel due to the approximately constant heat transfer to the desiccant for regeneration.

The desiccant regeneration rate and efficiency strongly depend on the temperature of the desiccant at the air-desiccant interface. This temperature needs to be maintained by constant heat transfer from the hot water and air to the desiccant. Most of the heat transfer to the desiccant is from the water due to the higher thermal conductivity of water. Thus to increase the regeneration rate, the water that is supplied to the regenerator must have both a high temperature and a high thermal capacitance rate. This can explain the decrease in regeneration efficiency when $R_{\dot{m}cp}$ is low for the very low $(\dot{m}c_p)_{total}$ of $5\text{W/m}^2\text{K}$. It can be observed that even though the thermal capacitance rate of the water increases with a decrease in $R_{\dot{m}cp}$, the temperature of water supplied decreases rapidly due to convection losses at the front of the collector, leading to a drop in the regeneration efficiency.

The efficiency of the optimized combined LATSC-LDR system was found to be 22.59%. This is comparable to the efficiency 20-30% (Jones and Harrison, 2008) of a liquid desiccant regenerator which is provided low grade thermal energy from a flat plate collector. However in this case the system cost is lower because the low cost of the unglazed collector is the main determinant of system cost.

7. Conclusion

A simple numerical model of a falling film type liquid desiccant regenerator has been developed and coupled with the numerical model of the LATSC. A sensitivity analysis is first performed on the combined system to assess the change in performance of the combined system to variations in $(\dot{m}c_p)_{total}$ and $R_{\dot{m}cp}$. It was observed that the collector efficiency tends to increase with higher $(\dot{m}c_p)_{total}$ and $R_{\dot{m}cp}$. The regeneration efficiency on the other hand tends to decrease with an increase in $(\dot{m}c_p)_{total}$ and $R_{\dot{m}cp}$ except at very low flow rates. The overall system efficiency therefore exhibits an optimum $R_{\dot{m}cp}$ for each $(\dot{m}c_p)_{total}$. This optimum $R_{\dot{m}cp}$ value decreases as $(\dot{m}c_p)_{total}$ increases, indicating that the system only requires a critical air flow rate to suppress the majority of the convection losses.

The combined LASTC-LDR system was optimized for typical Abu Dhabi conditions. The aim was to determine the values of the thermal capacitance rates of air and water and the desiccant mass flow rate which provides optimum performance of the system. For the typical Abu Dhabi conditions it was found that the optimum water thermal capacitance rate, air thermal capacitance rate, desiccant mass flow rate per unit regenerator area and desiccant mass flow rate per unit collector area are $38.655\text{ W/m}^2\text{K}$, $10.979\text{ Wm}^2\text{K}$, $0.0003329\text{ kg/s-m}^2$ and $0.00016645\text{ kg/s-m}^2$ respectively. The optimized system efficiency was found to be 22.59%.

Nomenclature

A	Collector area (m^2)
C_a	Concentration of water in air (kg_w/kg_a)
C_d	Concentration of water in desiccant (kg_w/kg_d)
C_{int}	Equilibrium concentration of water at air-desiccant interface (kg_w/kg_d)
c_{pa}	Specific heat of air (kJ/kgK)
c_{pw}	Specific heat of water (kJ/kgK)

D_a	Mass diffusivity (m^2/s)
D_p	Hydraulic diameter of plenum (m)
G	Absorbed solar radiation (W/m^2)
h_a	Air heat transfer coefficient (W/m^2K)
h_{fg}	Latent heat of vaporization of water(kJ/kg)
h_m	Mass transfer coefficient of water vapor (kg/m^2s)
h_w	Water heat transfer coefficient (W/m^2K)
k	Thermal conductivity (W/mK)
L	Length of collector (m)
$(\dot{m}c_p)_{total}$	Total thermal capacitance rate of air and water
\dot{m}	Mass flow rate (kg/s)
$R_{\dot{m}c_p}$	Ratio of $\dot{m}c_{p_{air}}$ to $\dot{m}c_{p_{total}}$
Nu	Nusselt's number
q_a	Convection rate at air-desiccant interface per unit area(W/m^2)
q_{back}	Convection to air in back channel per unit area(W/m^2)
$q_{back,loss}$	Back convection loss per unit area(W/m^2)
$q_{conv,loss}$	Convection loss per unit area(W/m^2)
q_{edge}	Edge Loss per unit area of the collector(W/m^2)
$q_{rad,loss}$	Radiation loss per unit area (W/m^2)
q_w	Convection rate at water-desiccant interface per unit area(W/m^2)
$q_{c,air}$	Heat transferred to suction air per unit area (W/m^2)
Q_u	Useful energy transferred to water (W)
Re	Reynold's Number
T_a	Air temperature (K)
T_{amb}	Ambient temperature (K)
T_d	Desiccant temperature (K)
T_{pl}	Plate temperature (K)
T_w	Water Temperature (K)
W	Width of collector (m)
x	lateral distance from tube(m)
y	distance from inlet end of collector(m)

Greek letters:

ε_{hx}	Heat exchange effectiveness of perforated plate
ρ	Density (kg/m^3)
ω	Humidity ratio of air (kg_w/kg_{da})

Subscripts:

a	air
d	desiccant
da	dry air
ds	desiccant salt
i	inlet
o	outlet
reg	regenerator
tot	air +water
w	water
wd	water in desiccant
wv	water vapor

Acknowledgement

The authors are grateful to the Government of Abu Dhabi for funding this research through the Masdar Initiative. Thanks to Drs. Shamim and Afshari for helpful comments. To Dr. Mekias for help with the multi-core work station, EES and MATLAB setup. And Profs. Klein & Beckman for help with EES.

References

ASHRAE Handbook - Fundamentals (SI Edition), American Society of Heating, Refrigerating and Air-Conditioning Engineers, Inc., 2009.

Ali, M.T., et al., A Cooling Change-Point Model of Community-Aggregate Electrical Load, *Energy and Buildings*, 43 (2011) 28-37.

Armstrong, P.R., et al., Efficient Low-Lift Cooling with Radiant Distribution, Thermal Storage, and Variable-Speed Chiller Controls— Part I: Component and Subsystem Models, *HVAC&R RESEARCH*, 15 (2009) 366-400.

Burch, J., et al., Low-cost solar domestic hot water systems for mild climates, in: DOE Solar Energy Technologies Program Review Meeting, Denver, Colorado, Denver, Colorado, 2005.

Conde, M.R., Properties of aqueous solutions of lithium and calcium chlorides: formulations for use in air conditioning equipment design, *International Journal of Thermal Sciences*, 43 (2004) 367-382.

Hyland, Wexler, Formulations for the thermodynamic properties of the saturated phases of H₂O from 173.15 K to 473.15 K, *ASHRAE Transactions, Part 2A* (1983).

Incropera, et al., *Fundamentals of Heat and Mass Transfer*, Wiley, 2006.

Jones, B.M., Harrison, S.J., First results of a solar-thermal liquid desiccant air conditioning concept, in: EURO SUN 2008 Lisbon Portugal 2008.

Kutscher, C.F., et al., Unglazed transpired solar collectors: heat loss theory, *Journal of Solar Energy Engineering*, 115 (1993) 182-188.

Lof, G.O.G., Cooling with solar energy, in: *World Symposium on Applied Solar Energy*, Phoenix, Arizona, 1956.

Qadir, A., Armstrong, P., Liquid-Air Transpired Solar Collector: Model Development and Sensitivity Analysis (in review), *Journal of Solar Energy Engineering*, (2011).

Remund, J., et al., METEONORM, in, Meteotest Bern, Switzerland, 2003.

Threlkeld, J.L., et al., *Thermal Environmental Engineering*, Prentice-Hall, 1998.